Available online at www.sciencedirect.com
SCIENCE DIRECT®
ELSEVIER
International Journal of Solids and Structures 43 (2006) 2351–2363
INTERNATIONAL JOURNAL OF SOLIDS and STRUCTURES
www.elsevier.com/locate/ijsolstr

Deformability of thin metal films on elastomer substrates

Teng Li, Z. Suo *

Division of Engineering and Applied Sciences, Harvard University, Cambridge, MA 02138, USA

Received 6 January 2005; received in revised form 6 April 2005
Available online 9 June 2005

Abstract

Recent applications in flexible electronics require that thin metal films grown on elastomer substrates be deformable. However, how such laminates deform is poorly understood. While a freestanding metal film subject to tension will rupture at a small strain by undergoing a necking instability, we anticipate that a substrate will retard this instability to an extent that depends on the relative stiffness and thickness of the film and the substrate. Using a combination of a bifurcation analysis and finite element simulations, we identify three modes of tensile deformation. On a compliant elastomer, a metal film forms a neck and ruptures at a small strain close to that of a freestanding film. On a stiff elastomer, the metal film deforms uniformly to large strains. On an elastomer of intermediate compliance, the metal film forms *multiple necks*, deforms much beyond the initial bifurcation, and ruptures at a large strain. Our theoretical predictions call for new experiments.

Keywords: Rupture; Metal film; Elastomer substrate; Necking; Bifurcation

1. Introduction

Flexible electronics are being developed for diverse applications, such as paper-like displays that can be folded or rolled (Forrest, 2004), electronic skins for humans and robots (Wagner et al., 2005), and sensors to monitor soft tissues (Gray et al., 2004). In some designs, small islands of stiff materials and thin metal interconnects are deposited on a polymer substrate. When the structure is stretched, the islands strain negligibly, but the metal interconnects deform with the substrate. Mechanical failure, such as rupture and debond of metal interconnects, poses a significant challenge.

* Corresponding author. Tel.: +1 617 4953789; fax: +1 617 4960601.
E-mail address: suo@deas.harvard.edu (Z. Suo).

0020-7683/$ - see front matter © 2005 Elsevier Ltd. All rights reserved.
doi:10.1016/j.ijsolstr.2005.04.034

A metal film, patterned in a zig-zag shape and embedded in a polymer substrate, acts like a spring, and can sustain a large elongation of the substrate (Gray et al., 2004). Nonetheless, such a structure still fails by rupture of the metal at sites of strain concentration. In this paper, to study the basic behavior of rupture, we focus on a blanket film on a polymer substrate. Experiments have shown that a freestanding thin metal film usually ruptures at a small strain (~1%; Pashley, 1960; Baral et al., 1984; Keller et al., 1996; Huang and Spaepen, 2000; Xiang et al., 2002; Espinosa et al., 2003; Lee et al., 2003). By contrast, thin metal films on polymer substrates rupture at strains of a large disparity, ranging from less than one percent to a few tens of percent (Chiu et al., 1994; Kang, 1996; Macionczyk and Bruckner, 1999; Kraft et al., 2000; Hommel and Kraft, 2001; Gage and Phanitsiri, 2001; Alaca et al., 2002; Yu and Spaepen, 2003; Lacour et al., 2003; Gruber et al., 2003; Xiang et al., 2005).

An essential difference between a freestanding and a substrate-bonded metal film is appreciated as follows (Fig. 1). The low ductility of a freestanding metal film results from local thinning. For a sufficiently thin metal film, dislocations readily escape from the surfaces of the film. Subsequently, the metal film does not harden appreciably. Even for a metal film passivated by a native oxide or other hard coatings, a modest strain will break the coatings and allow dislocations to escape. Without hardening, the tensile deformation of a freestanding metal film is unstable: a perturbation in its thickness promotes the film to thin down locally, and a single neck causes the film to rupture. By volume conservation, upon rupture, the local thinning causes a local elongation on the order of the film thickness. Given the small thickness-to-length ratio of the film, this local elongation contributes little to the overall rupture strain.

The local elongation requires space to accommodate. This space is available to the freestanding film as the ruptured halves move apart, but is unavailable to the film bonded to a substrate subject to a modest tensile strain. Consequently, the polymer substrate may delocalize the strain field in the metal film, carrying the film far beyond the rupture strain of a freestanding film. The large rupture strains of metal films bonded to polyimide substrates have been demonstrated in experiments (Kang, 1996; Macionczyk and Bruckner, 1999; Gruber et al., 2003; Xiang et al., 2005), and in our finite element simulations (Li et al., 2005). Our simulations have also shown that, once debonded from the substrate, the metal film behaves just like a freestanding film, rupturing at a small strain. We believe that the observed disparity in the rupture strains of the metal films on polymer substrates is caused, at least in part, by the disparity in the quality of bonding.

Our previous paper (Li et al., 2005) has focused on metal films on a relatively stiff polymer (polyimide). Applications such as electronic skins require much more compliant substrate material, such as silicone. A question remains whether such an elastomer substrate can still carry a metal film to large strains. A

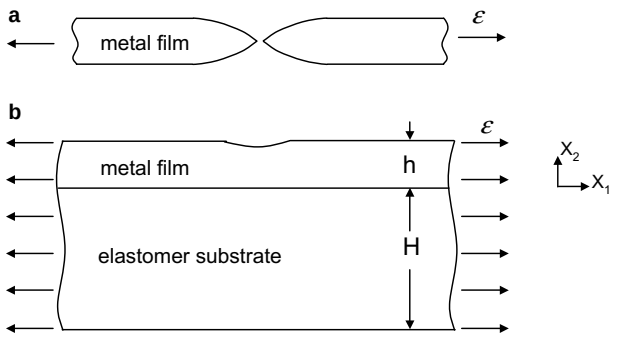

Fig. 1. When a metal film ruptures, local thinning leads to a local elongation. (a) A freestanding metal film accommodates the local elongation as the ruptured halves move apart and (b) a substrate-bonded film cannot accommodate the local elongation, so that the strain field in the metal film is delocalized, allowing the film to deform to large strains.

preliminary study shows that an elastomer substrate may do so by stabilizing *multiple necks* in the metal film (Li et al., 2004).

The present paper reports an extended study of the deformability of metal/elastomer laminates. When the applied strain is small, the laminates deform uniformly (Section 2). At some critical strains, subject to a perturbation of small amplitude, the uniform deformation bifurcates into nonuniform deformation (Section 3). Using finite element simulations, we study large-amplitude nonuniform deformation of the laminates (Section 4). Provided the substrates are not too compliant, we find that the metal films can deform substantially after the initial bifurcation, and rupture at strains much larger than the critical strains at which bifurcation sets in.

2. Stability of uniform deformation against perturbations of long wavelengths

As a freestanding metal loaded in tension elongates in one direction and thins in the transverse direction, the tensile force increases due to the hardening of the metal, but decreases due to the reduction in the cross-sectional area. The tensile force peaks at some strain, at which a neck sets in. The uniform deformation in the metal becomes unstable when the geometric softening prevails over material hardening. This model is attributed to Considère in textbooks. By contrast, the same model shows that the uniform deformation in a freestanding elastomer is stable for all strains, because the elastomer stiffens so steeply that the tensile force always increases with deformation. What will happen to a metal/elastomer laminate?

Fig. 1 illustrates the model. A blanket metal film, initial thickness h, is bonded to an elastomer substrate, initial thickness H. The metal film is modeled by the J_2 deformation theory; under uniaxial tension, the metal deforms according to the power law $\sigma = K\varepsilon^N$, where σ is the true stress, ε the strain, K the pre-factor, and N the hardening exponent. The elastic strain in the metal is neglected. This paper uses the natural strain as the strain measure, defined by the logarithm of the deformed length divided by the undeformed length. The elastomer is modeled as a Neo-Hookean solid (Treloar, 1948); under uniaxial tension, the elastomer deforms according to $\sigma = (E/3)(\exp(2\varepsilon) - \exp(-\varepsilon))$, where E is Young's Modulus. We assume that the laminate deforms under the plane strain conditions in the plane (x_1, x_2), subject to the applied strain ε in the x_1 direction.

We first study the uniform deformation of the laminate. Under the plane strain conditions, the stress in the x_1 direction relates to the applied strain as

$$\sigma_{\text{film}} = K(2/\sqrt{3})^{N+1}\varepsilon^N \tag{1}$$

in the film, and as

$$\sigma_{\text{sub}} = (2E/3)\sinh(2\varepsilon) \tag{2}$$

in the substrate. By volume conservation, as the laminate elongates in the x_1 direction, both the film and the substrate thin by a factor of $\exp(-\varepsilon)$ in the x_2 direction. Consequently, the resultant force in the x_1 direction is $F = (\sigma_{\text{film}}h + \sigma_{\text{sub}}H)\exp(-\varepsilon)$, or

$$\frac{F}{Kh} = \left[\left(\frac{2}{\sqrt{3}}\right)^{N+1}\varepsilon^N + \frac{2}{3}\sinh(2\varepsilon)\frac{EH}{Kh}\right]\exp(-\varepsilon). \tag{3}$$

Note that a single dimensionless parameter, EH/Kh, emerges here to quantify the effect of the substrate.

Fig. 2 plots the resultant force as a function of the applied strain ε. When $EH/Kh = 0$, the metal film is in effect freestanding; the resultant force first rises, peaks at a small strain, and then drops. When $EH/Kh > 0$, the resultant force scales as $F \sim \exp(\varepsilon)$ for large strains; consequently, even if the force peaks at a modest

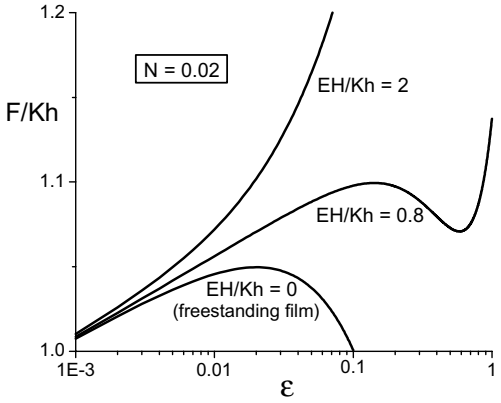

Fig. 2. When the laminate deforms uniformly, the force–strain relation exhibits three kinds of behaviors, depending on the parameters EH/Kh and N.

strain and then drops, the force will reach a minimum and increase again at larger strains. When EH/Kh is very large, the force increases monotonically for all strains.

Eqs. (1) and (2) describe a state of uniform deformation in the laminate. We now begin to study the stability of the uniform deformation against a perturbation of small amplitude. A Fourier component of the perturbation is sinusoidal in x_1, and has a wave number k (i.e., a wavelength $2\pi/k$). When the wavelength of the perturbation is much larger than the total thickness of the laminate, the laminate can be viewed as a series of segments along its length, each segment being in a state of uniform deformation. By force balance, all the segments carry the same resultant force. If the force–strain curve is not monotonic, the same force may correspond to two or three strains (Fig. 2). Such a force–strain curve allows the laminate to deform in a nonuniform state.

Setting $\mathrm{d}F/\mathrm{d}\varepsilon = 0$, we obtain from Eq. (3) that

$$\frac{EH}{Kh} = 3\left(\frac{2}{\sqrt{3}}\right)^{N+1} \frac{\varepsilon^{N-1}(\varepsilon - N)}{\exp(2\varepsilon) + 3\exp(-2\varepsilon)}. \tag{4}$$

When $EH/Kh = 0$, Eq. (4) recovers the well-known result that, for a freestanding metal, at the strain $\varepsilon = N$, the uniform deformation bifurcates into nonuniform deformation of a wavelength much larger than the film thickness. For a laminate, Eq. (4) divides the plane $(\varepsilon, EH/Kh)$ into two regions (Fig. 3). Above the curve, the force increases as the strain increases, $\mathrm{d}F/\mathrm{d}\varepsilon > 0$; below, $\mathrm{d}F/\mathrm{d}\varepsilon < 0$. The left part of the curve in Fig. 3 corresponds to the force maxima in Fig. 2; and the right part, the force minima. When the laminate is subject to a perturbation of a wavelength much larger than the total thickness of the laminate, uniform deformation is stable for all strains if $EH/Kh > 0.92$, and for strains up to the left part of the curve if $EH/Kh < 0.92$.

In the above, we have only considered perturbations of long wavelengths. In reality, a perturbation has Fourier components of all wavelengths. For each component, there is a critical strain at which the uniform deformation becomes unstable. The uniform deformation is stable against perturbation of all wavelengths if the applied strain is below the lowest critical strain. For a freestanding film, the lowest critical strain occurs at long wavelengths (Hill and Hutchinson, 1975). Consequently, it is a common practice to identify the long wave limit, $\varepsilon = N$, as the rupture strain of a freestanding metal. However, for a metal film on a thick elastomer (i.e., a large value of EH/Kh), the long wave limit of the critical strain given by Eq. (4) tends to infinity, so that the lowest critical strain occurs at a finite wavelength. We next study the stability of uniform deformation in the laminate against perturbations of all wavelengths.

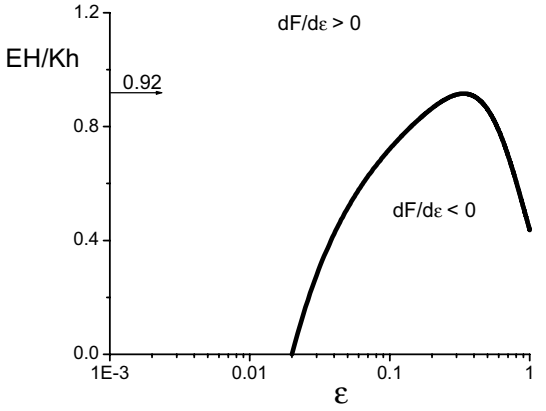

Fig. 3. For a given value of the hardening exponent ($N = 0.02$ used in this plot), the plane of ε and EH/Kh is divided into two regions: above the curve, $\mathrm{d}F/\mathrm{d}\varepsilon > 0$; below, $\mathrm{d}F/\mathrm{d}\varepsilon < 0$. Uniform deformation in the laminate is stable against perturbation of long wavelengths for all strains if $EH/Kh > 0.92$, and for strains up to the left part of the curve if $EH/Kh < 0.92$.

3. Stability of uniform deformation against perturbations of all wavelengths

We perform the bifurcation analysis using an established procedure (e.g., Hill and Hutchinson, 1975; Stören and Rice, 1975; Dorris and Nemat-Nasser, 1980; Rivlin, 1982; Steif, 1986; Bigoni et al., 1997; Shenoy and Freund, 1999). This procedure is summarized here for the laminate. Take the current state of uniform deformation, defined by Eqs. (1) and (2), as the reference state. Represent a nonuniform perturbation by a small increment in the displacement field $v_i(x_1, x_2)$, and a small increment in the nominal stress field $\dot{T}_{ij}(x_1, x_2)$. The increments are in equilibrium and incompressible:

$$\dot{T}_{ij,i} = 0, \quad v_{i,i} = 0. \tag{5}$$

For either the metal film or the elastomer substrate, the constitutive law takes the form (Hill and Hutchinson, 1975):

$$\begin{aligned}
\dot{T}_{11} &= (\mu_* - \sigma)v_{1,1} - \mu_* v_{2,2} + \dot{p},\\
\dot{T}_{22} &= \mu_*(v_{2,2} - v_{1,1}) + \dot{p},\\
\dot{T}_{12} &= \left(\mu + \frac{\sigma}{2}\right)v_{2,1} + \left(\mu - \frac{\sigma}{2}\right)v_{1,2},\\
\dot{T}_{21} &= \left(\mu - \frac{\sigma}{2}\right)(v_{2,1} + v_{1,2}),
\end{aligned} \tag{6}$$

where $\dot{p}$ is the increment in the mean stress. For the metal film, σ is given by Eq. (1), $\mu = (K/2)\varepsilon^N \coth(2\varepsilon)$ and $\mu_* = (KN/4)\varepsilon^{N-1}$. For the elastomer substrate, σ is given by Eq. (2), and $\mu = \mu_* = (E/3)\cosh(2\varepsilon)$.

A Fourier component of the perturbation takes the form

$$v_1 = a_1 \mathrm{e}^{\mathrm{i}kx_1 + \tau x_2}, \quad v_2 = a_2 \mathrm{e}^{\mathrm{i}kx_1 + \tau x_2}, \quad \dot{p} = c\mathrm{e}^{\mathrm{i}kx_1 + \tau x_2}, \tag{7}$$

where k is the wave number, $i = \sqrt{-1}$, and a_1, a_2, c and τ are constants. A substitution of (6) and (7) into (5) leads to

$$\begin{bmatrix} (\mu - \sigma/2)\tau^2 - (\mu_* - \sigma)k^2 & \mathrm{i}\tau k(\mu - \mu_* - \sigma/2) & \mathrm{i}k \\ \mathrm{i}\tau k(\mu - \mu_* - \sigma/2) & \mu_*\tau^2 - (\mu + \sigma/2)k^2 & \tau \\ \mathrm{i}k & \tau & 0 \end{bmatrix} \begin{bmatrix} a_1 \\ a_2 \\ c \end{bmatrix} = 0. \tag{8}$$

This is a set of linear algebraic equations for a_1, a_2 and c. To have nontrivial solutions, the determinant of (8) must vanish, which gives four roots:

$$\tau_{1,2} = \pm k\sqrt{\frac{2\mu - 4\mu_* + \Lambda}{-2\mu + \sigma}}, \quad \tau_{3,4} = \pm k\sqrt{\frac{2\mu - 4\mu_* - \Lambda}{-2\mu + \sigma}} \tag{9}$$

with $\Lambda = \sqrt{\sigma^2 - 16\mu_*(\mu - \mu_*)}$. In general, the roots in (9) are complex-valued, as discussed by Hill and Hutchinson (1975). Assuming all roots are distinct, a general representation of the perturbation is

$$\begin{aligned} v_1 &= \mathrm{e}^{\mathrm{i}kx_1}(b_1\mathrm{e}^{\tau_1 x_2} + b_2\mathrm{e}^{-\tau_1 x_2} + b_3\mathrm{e}^{\tau_3 x_2} + b_4\mathrm{e}^{-\tau_3 x_2}), \\ v_2 &= \mathrm{i}\mathrm{e}^{\mathrm{i}kx_1}\left[\frac{\tau_1}{k}(b_1\mathrm{e}^{\tau_1 x_2} - b_2\mathrm{e}^{-\tau_1 x_2}) + \frac{\tau_3}{k}(b_3\mathrm{e}^{\tau_3 x_2} - b_4\mathrm{e}^{-\tau_3 x_2})\right], \\ \dot{p} &= \mathrm{e}^{\mathrm{i}kx_1}\left[\frac{\tau_1(\Lambda - \sigma)}{2}(b_1\mathrm{e}^{\tau_1 x_2} - b_2\mathrm{e}^{-\tau_1 x_2}) - \frac{\tau_3(\Lambda + \sigma)}{2}(b_3\mathrm{e}^{\tau_3 x_2} - b_4\mathrm{e}^{-\tau_3 x_2})\right], \end{aligned} \tag{10}$$

where b_1, b_2, b_3, b_4 are constants. Eq. (10) is applicable to both the film and the substrate, but with different sets of constants, denoted as τ_i^+, b_i^+ for the film, and τ_i^-, b_i^- for the substrate.

There are eight boundary conditions for the laminate: two tractions vanish at the top surface of the film, two tractions vanish at the bottom surface of the substrate, and two tractions and two displacements are continuous at the interface. These boundary conditions lead to a set of homogeneous algebraic equations for b_1^+, b_2^+, b_3^+, b_4^+, b_1^-, b_2^-, b_3^-, b_4^-, with the coefficient matrix $\mathbf{L}$ given in Appendix A. To have nontrivial solutions, the determinant of the matrix must vanish, $\det(\mathbf{L}) = 0$. This equation determines the critical strain for a given wave number.

We now describe the critical strains calculated from the above procedure. First consider a freestanding metal film. In the long wave limit, $kh \to 0$, the Considère model gives the critical strain $\varepsilon = N$. In the short wave limit, $kh \to \infty$, the nonuniform deformation develops near the surfaces of the layer, and decays exponentially in the thickness direction of the film; the bifurcation analysis gives critical strain $\varepsilon \approx \sqrt{N/2}$ for small N. Fig. 4 includes a plot of the critical strain as a function of kh for the freestanding metal film. For $N = 0.02$, the curve approaches the long wave limit $\varepsilon = 0.02$ and the short wave limit $\varepsilon = 0.105$.

Next consider the metal/elastomer laminate, which is characterized by three dimensionless parameters: E/K, H/h and N. In numerical examples, we will model the metal as a weakly hardening material, $N = 0.02$ and $K = 114$ MPa. We will vary Young's modulus of the elastomer, $E = 20$, 120, 200 MPa (corresponding

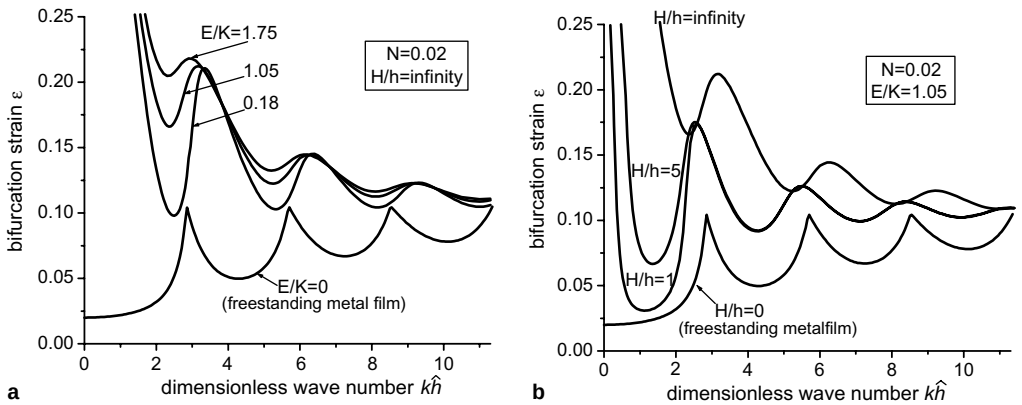

Fig. 4. The critical strains at which uniform deformation becomes unstable are plotted as a function of the wave number of the perturbation, for substrates of various elastic moduli (a), and of various thicknesses (b).

to $E/K = 0.18$, 1.05, 1.75, respectively). We will also vary the thickness ratio, $H/h = 0$ (freestanding metal film), 1, 5, 50. Fig. 4 compares the critical strain of the laminate to that of the freestanding metal film. In the short wave limit, $kh \to \infty$, the perturbation does not sense the existence of the substrate, and the critical strain corresponds to the short wave limit of the freestanding metal film. In the long wave limit, $kh \to 0$, the critical strain is given by Eq. (4), being infinite for the parameters chosen in Fig. 4. The critical strain drops precipitously as the wavelength of the perturbation decreases. The presence of the elastomer substrate elevates the critical strain: the stiffer the substrate, the higher the critical strain (Fig. 4a). Similarly, the thicker the substrate, the higher the critical strain (Fig. 4b).

The previous two sections study small perturbations from uniform deformation. The following considerations motivate the need to study nonuniform deformation of large amplitudes.

For a metal film on a stiff substrate, the lowest critical strain occurs at a small wavelength. Recall that the short wave limit of the laminate is the same as that of the freestanding metal film, $\varepsilon \approx \sqrt{N/2}$. Do these results mean that, a nonhardening metal film on a stiff substrate will rupture at very small strains? The answer is no. For the film to rupture at a small wavelength, to accommodate elongations associated with closely spaced necks, a large strain must be applied to the substrate.

For a metal film on a compliant substrate, the lowest critical strain occurs at a wavelength several times the film thickness, and is not much above the long wave limit of a freestanding film, $\varepsilon = N$. Upon further straining, will such nonuniform deformation amplify to grow multiple necks, or will deformation localize to grow a single neck? The former would lead to a large rupture strain, and the latter a small rupture strain. We expect that the outcome depends on how compliant the substrate is.

4. Large-amplitude nonuniform deformation

The questions raised in the last two paragraphs suggest that, for a metal/elastomer laminate, the critical strain at which bifurcation sets in can be very different from the strain at which the film ruptures. To answer the above questions quantitatively, we must analyze large-amplitude nonuniform deformation in the laminate. We do so by using the finite element code ABAQUS.

To initiate nonuniform deformation in the finite element simulations, we place a V-shaped notch, 0.2 h wide and 0.05 h deep, at the center of the film surface. Three-node triangular elements are used in the film, four-node quadrilateral elements in the substrate, and matching elements along the interface. The size of the element along the interface is 0.1 h and a comparable element size is used in the whole film, except for the region near the notch, where the meshes are dense. Coarser elements are used in the part of substrate far away from the interface.

Simulation results are shown for films on substrates of various elastic moduli and thicknesses, Fig. 5 ($H/h = 50$), Fig. 6 ($H/h = 5$), and Fig. 7 ($H/h = 1$). Depending on the elastic modulus of the substrate, three modes of deformation can be identified. As the first mode of deformation, when the substrate is very compliant (e.g., $E/K = 0.18$), the film forms a single neck near the preexisting notch, and the substrate locally distorts to follow the neck in the film. The notch starts thinning at a strain of about 0.02, and the film ruptures at a strain comparable to that of a freestanding film. As expected, the very compliant substrate does not delocalize the strain field in the metal film.

As the second mode of deformation, when the substrate is of intermediate stiffness (e.g., $E/K = 1.05$), the film forms multiple necks, stretches to a *much higher strain*, and then ruptures near the preexisting notch. The spacing between the necks is comparable to the wavelength corresponding to the lowest critical strain, but the rupture strain is much larger than the critical strain for the nonuniform deformation to set in. For example, the bifurcation analysis predicts that the lowest critical strain occurs at $kh = 1.36$, 1.35 and 1.08 for, respectively, $H/h = 50$, 5 and 1, while the corresponding finite element simulations show that $kh = 1.65$, 1.60 and 0.97. The fair agreement indicates that the perturbation at the wavelength corresponding to the

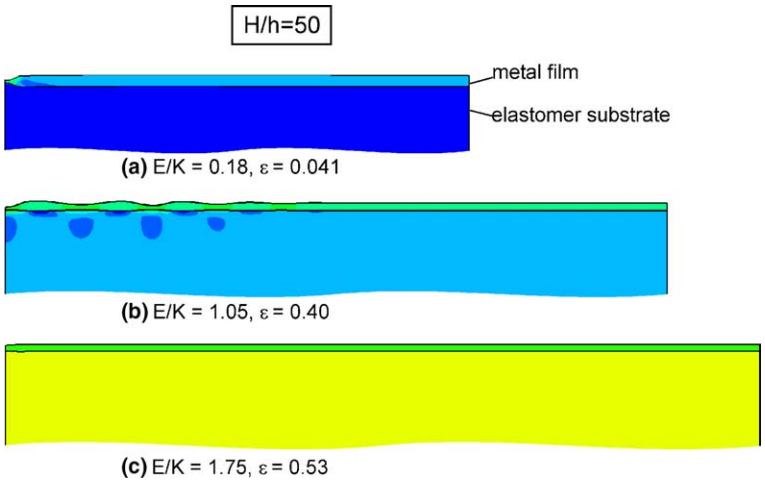

Fig. 5. Finite element simulations identify three modes of tensile deformation, depending on the stiffness of the substrate. The substrates are thick ($H/h = 50$). The right half of the laminate and only part of the substrate are shown. Contours represent the Mises stress level. Note the much larger strains of the last two modes.

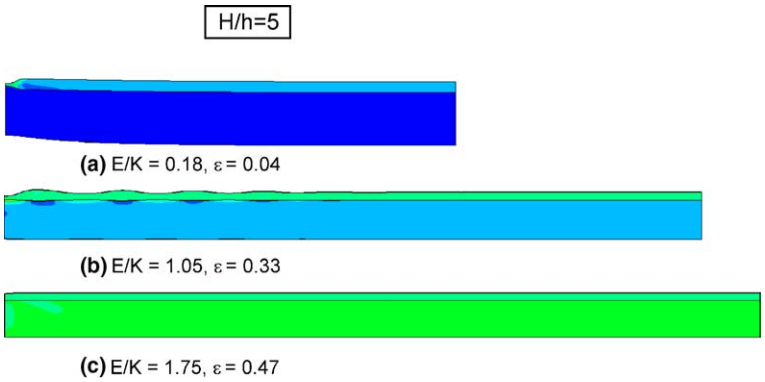

Fig. 6. Three modes of tensile deformation of the metal films on thin substrates ($H/h = 5$). Note the much larger strains of the last two modes.

lowest critical strain prevails over those of other wavelengths, and sets the spacing of the multiple necks. Further deformation involves the elongation of the film and the distortion of the substrate near all necks. Each neck contributes an extra elongation. As a whole, the metal film can stretch to a large strain before final rupture. Further simulations show that this significant increase in the rupture strain of the metal film is insensitive to the size of the preexisting notch. Multiple necks stabilize on substrates of a range of stiffness ($E = 80$–160 MPa). The stiffer the substrate, the smaller the spacing between the necks, and the larger the rupture strain.

As the third mode of deformation, when the substrate is stiff (e.g., $E/K = 1.75$), the metal film can deform uniformly to large strains. The lowest critical strain occurs at small wavelengths, close to the short wave limit for a freestanding metal film. Further growth of such short wave perturbations to rupture involves huge local strain. The metal film deforms nearly uniformly to a large strain without rupture, even

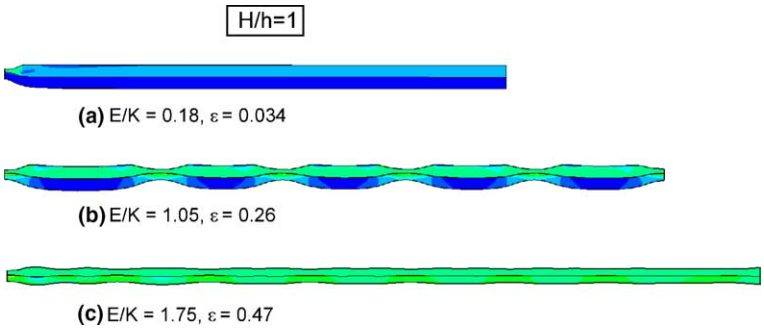

Fig. 7. Three modes of tensile deformation of the metal films on very thin substrates ($H/h = 1$). The last two modes still lead to much larger strain.

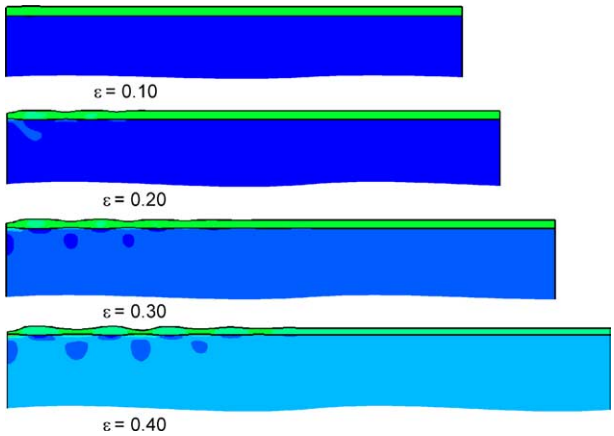

Fig. 8. A sequence of deformed states of a laminate with $E/K = 1.05$ and $H/h = 50$. Note the formation of multiple necks in the film.

at the preexisting notch. This behavior is similar to that of a metal film on a polyimide substrate (Li et al., 2005).

Fig. 8 shows a sequence of snapshots of deformation leading to multiple necks ($H/h = 50$, $E/K = 1.05$). At small strains, the film deforms uniformly; the preexisting notch does not cause any significant nonuniformity in the deformation. At large strains, nonuniform deformation becomes pronounced, and develops into multiple necks. The film eventually ruptures near the notch.

To see how a very thin elastomer substrate stabilizes multiple necks in a metal film, Fig. 9 plots the resultant forces in the film, F_{film}, and in the substrate, F_{sub}, extracted from the finite element simulations, for cases of $H/h = 1$ and various elastic moduli. For the laminate with $E/K = 0.18$, the total force keeps decreasing as the applied strain increases. The total force drops abruptly when the neck sets in. For the laminate with $E/K = 1.05$, the abrupt drop in F_{film} due to film necking is compensated by an abrupt increase in F_{sub}. The total force keeps nearly constant. The Neo-Hookean material stiffens substantially at large strain. As a result, the elastomer becomes so stiff near each neck that it impedes the necking development. The necking of metal film on a sufficiently stiff elastomer is *stable*. For the laminate with $E/K = 1.75$, the total force keeps increasing as applied strain increases, indicating stable stretching of the laminate without forming necks.

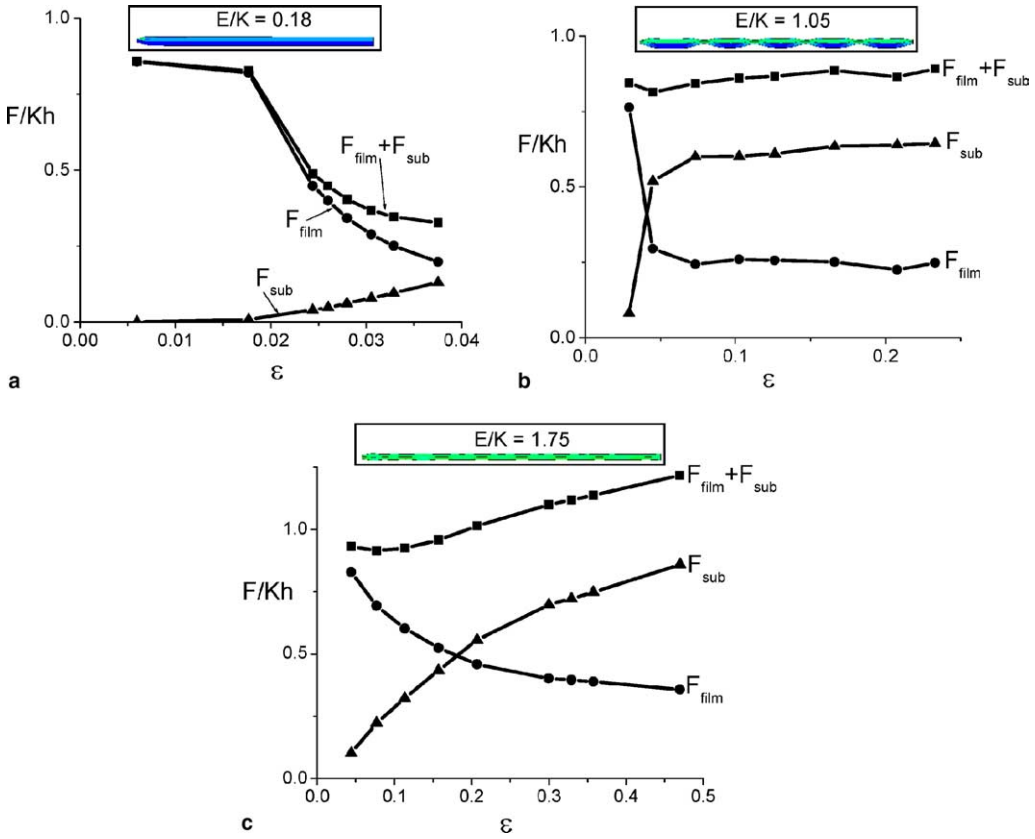

Fig. 9. Resultant forces in x_1 direction in the laminates ($H/h = 1$) as a function of the applied tensile strain. $E/K = 0.18$ in (a), 1.05 in (b), 1.75 in (c). All data points are extracted from the finite element simulations.

5. Discussions

Multiple necks have been observed in several situations. For example, when a metal ring is expanded at a high strain rate using electromagnetic loading, after a period of nearly uniform deformation, the ring forms multiple necks (Niordson, 1965). Inertia suppresses the rates of growth of both very long and very short wavelength modes of nonuniform deformation, promoting multiple necks at an intermediate wavelength (Shenoy and Freund, 1999). As another phenomenon, multiple shear bands have been observed in metallic glass layers sandwiched between two ductile metal layers (Alpas and Embury, 1988). When a shear band forms in the metallic glass, the ductile metal layers arrest the shear band, so that the stress in the metallic glass away from the shear band is kept high, allowing new shear bands to form. While the role of inertia or the ductile metal layers is analogous to that of the elastomer substrate, we are unaware of any experimental observation of multiple necks in thin metal films on elastomer substrates. Our theoretical prediction therefore calls for new experiments.

In the present model, we assume perfect bonding between the metal film and the elastomer substrate. In practice, the metal/elastomer interface is never perfect. When such a structure is stretched, debond may occur, so that the metal film becomes freestanding and ruptures at a small strain. The debond on the interface and the necking in the film may develop simultaneously, facilitating each other. In this sense, the present

model may overestimate the rupture strain of the metal films. We will report simulations of the co-evolution of debond and necking elsewhere.

We assume that the laminate deforms under the plane strain conditions; for example, the preexisting notch in the simulations corresponds to an infinitely long trench in the film surface. In a real metal film, an imperfection such as a missing grain may initiate nonuniform deformation, which then propagates across the film, leaving a long neck in its wake. Rupture by this process requires higher applied strain than that of the rupture originated by a long trench in the film. In this sense, the present model underestimates the rupture strain. (Begley and Bart-Smith (2005) have studied the formation of periodic cracks in thin metal films on elastomer substrates, but they have assumed that the metal films are elastic.) Another effect is not captured by the plane strain conditions. Under a tensile force, a laminate elongates in one direction and contracts in two other directions. The difference in Poisson's ratios in the metal and the elastomer causes in the metal film a compressive stress transverse to the applied force, causing the metal film to wrinkle. These effects will be studied elsewhere.

Our simulations assume that the metal films obey the J_2 deformation theory. In reality, the metal film is polycrystalline, with the grain size comparable to the film thickness. We have also assumed that the elastomer substrates allow dislocations to escape from the metal films, so that the metal films harden weakly at large strains. To what extent these assumptions reflect the reality is uncertain. Nonetheless, the constraint of the substrate on the film is largely geometrical, so that the prediction of enhanced rupture strain should stand, provided the metal film is plastically deformable and remains adherent to the substrate.

6. Summary

Under tension, the state of uniform deformation is unstable in a freestanding metal layer when the strain exceeds a critical value. By contrast, the state of uniform deformation is stable in a freestanding elastomer layer for all strains. This paper studies the behavior of a laminate of a metal film bonded on an elastomer substrate. We calculate the resultant force in the laminate under uniform deformation. When the resultant force as a function of the strain peaks, the uniform deformation gives in to a perturbation of a wavelength much larger than the total thickness of the laminate. This simple model tends to overestimate the effect of the substrate in stabilizing the uniform deformation, as the critical strain drops precipitously as the wavelength of the perturbation decreases. Using a bifurcation analysis, we study the stability of the uniform deformation of the laminate against perturbations of all wavelengths. When the substrate is stiff, the lowest critical strain approaches the short wave limit of the freestanding metal film. When the substrate is compliant, the lowest critical strain occurs at wavelengths about a few times the thickness of the film, and is not much above the long wave limit of the freestanding metal film. Simulations of large-amplitude nonuniform deformation show that, provided the substrate is not too compliant, the metal film can sustain strains much beyond the critical strain predicted by the bifurcation analysis. Such large rupture strains result from the formation of *multiple necks* in the film.

Acknowledgments

The work was supported by the National Science Foundation through the MRSEC at Harvard University, and by the Division of Engineering and Applied Sciences at Harvard University.

Appendix A

The components of the matrix **L** are

$$
\begin{aligned}
&L_{11} = A^+\tau_1^+ \exp(\tau_1^+\hat{h}), \quad L_{12} = -A^+\tau_1^+ \exp(-\tau_1^+\hat{h}),\\
&L_{13} = B^+\tau_3^+ \exp(\tau_3^+\hat{h}), \quad L_{14} = -B^+\tau_3^+ \exp(-\tau_3^+\hat{h}),\\
&L_{15} = L_{16} = L_{17} = L_{18} = 0,\\
&L_{21} = C^+ \exp(\tau_1^+\hat{h}), \quad L_{22} = C^+ \exp(-\tau_1^+\hat{h}),\\
&L_{23} = D^+ \exp(\tau_3^+\hat{h}), \quad L_{24} = D^+ \exp(-\tau_3^+\hat{h}),\\
&L_{25} = L_{26} = L_{27} = L_{28} = 0,\\
&L_{31} = A^+\tau_1^+, \quad L_{32} = -A^+\tau_1^+, \quad L_{33} = B^+\tau_3^+, \quad L_{34} = -B^+\tau_3^+,\\
&L_{35} = -A^-\tau_1^-, \quad L_{36} = A^-\tau_1^-, \quad L_{37} = -B^-\tau_3^-, \quad L_{38} = B^-\tau_3^-,\\
&L_{41} = L_{42} = C^+, \quad L_{43} = L_{44} = D^+,\\
&L_{45} = L_{46} = -C^-, \quad L_{47} = L_{48} = -D^-,\\
&L_{51} = -L_{52} = \tau_1^+, \quad L_{53} = -L_{54} = \tau_3^+,\\
&L_{56} = -L_{55} = \tau_1^-, \quad L_{58} = -L_{57} = \tau_3^-,\\
&L_{61} = L_{62} = L_{63} = L_{64} = 1, \quad L_{65} = L_{66} = L_{67} = L_{68} = -1,\\
&L_{71} = L_{72} = L_{73} = L_{74} = 0,\\
&L_{75} = A^-\tau_1^- \exp(-\tau_1^-\widehat{H}), \quad L_{76} = -A^-\tau_1^- \exp(\tau_1^-\widehat{H}),\\
&L_{77} = B^-\tau_3^- \exp(-\tau_3^-\widehat{H}), \quad L_{78} = -B^-\tau_3^- \exp(\tau_3^-\widehat{H}),\\
&L_{81} = L_{82} = L_{83} = L_{84} = 0,\\
&L_{85} = C^- \exp(-\tau_1^-\widehat{H}), \quad L_{86} = C^- \exp(\tau_1^-\widehat{H}),\\
&L_{87} = D^- \exp(-\tau_3^-\widehat{H}), \quad L_{88} = D^- \exp(\tau_3^-\widehat{H}),
\end{aligned}
$$

where

$$
\begin{aligned}
&A^\pm = 2\mu_*^\pm + (\Lambda^\pm - \sigma^\pm)/2,\\
&B^\pm = 2\mu_*^\pm - (\Lambda^\pm + \sigma^\pm)/2,\\
&C^\pm = (\mu^\pm - \sigma^\pm/2)(k + (\tau_1^\pm)^2/k),\\
&D^\pm = (\mu^\pm - \sigma^\pm/2)(k + (\tau_3^\pm)^2/k),\\
&\hat{h} = h\exp(-\varepsilon), \quad \widehat{H} = H\exp(-\varepsilon).
\end{aligned}
$$

References

Alaca, B.E., Saif, M.T.A., Sehitoglu, H., 2002. On the interface debond at the edge of a thin film on a thick substrate. Acta Mater. 50, 1197–1209.

Alpas, A.T., Embury, J.D., 1988. Flow localization in thin layers of amorphous alloys in laminated composite structures. Scripta Metall. 22, 265–270.

Baral, D., Ketterson, J.B., Hilliard, J.E., 1984. Mechanical properties of composition modulated Cu–Ni foils. J. Appl. Phys. 57, 1076–1083.

Begley, M.R., Bart-Smith, H., 2005. The electro-mechanical response of highly compliant substrates and thin stiff films with periodic cracks. Int. J. Solids Struct. 42, 5259–5273.

Bigoni, D., Ortiz, M., Needleman, A., 1997. Effect of interfacial compliance on bifurcation of a layer bonded to a substrate. Int. J. Solids Struct. 34, 4305–4326.
Chiu, S.L., Leu, J., Ho, P.S., 1994. Fracture of metal-polymer line structures. I. Semiflexible polyimide. J. Appl. Phys. 76, 5136–5142.
Dorris, J.F., Nemat-Nasser, S., 1980. Instability of a layer on a half space. J. Appl. Mech. 47, 304–312.
Espinosa, H.D., Prorok, B.C., Fischer, M., 2003. A methodology for determining mechanical properties of free-standing films and MEMS materials. J. Mech. Phys. Solids 51, 47–67.
Forrest, S.R., 2004. The path to ubiquitous and low-cost organic electronic appliances on plastic. Nature 428, 911–918.
Gage, D.M., Phanitsiri, M., 2001. Experimental and mathematical analysis of tensile fracture mechanics in thin-film metal deposits. Senior Thesis, Princeton University.
Gray, D.S., Tien, J., Chen, C.S., 2004. High-conductivity elastomeric electronics. Adv. Mater. 16, 393–397.
Gruber, P., Böhm, J., Wanner, A., Sauter, L., Spolenak, R., Arzt, E., 2003. Size effect on crack formation in Cu/Ta and Ta/Cu/Ta thin film systems. Mater. Res. Soc. Symp. Proc. 821, P2.7.
Hill, R., Hutchinson, J.W., 1975. Bifurcation phenomena in the plane tension test. J. Mech. Phys. Solids 23, 239–264.
Hommel, M., Kraft, O., 2001. Deformation behavior of thin copper films on deformable substrates. Acta Mater. 49, 3935–3947.
Huang, H., Spaepen, F., 2000. Tensile testing of free-standing Cu, Ag and Al thin films and Ag/Cu multilayers. Acta Mater. 48, 3261–3269.
Kang, Y.-S., 1996. Microstructure and Strengthening Mechanisms in Aluminum Thin Films on Polyimide Film. Ph.D. Thesis, supervised by P.H. Ho, The University of Texas at Austin.
Keller, R.R., Phelps, J.M., Read, D.T., 1996. Tensile and fracture behavior of free-standing copper films. Mater. Sci. Eng. A214, 42–52.
Kraft, O., Hommel, M., Arzt, E., 2000. X-ray diffraction as a tool to study the mechanical behavior of thin films. Mater. Sci. Eng. A288, 209–216.
Lacour, S.P., Wagner, S., Huang, Z.Y., Suo, Z., 2003. Stretchable gold conductors on elastomeric substrates. Appl. Phys. Lett. 82, 2404–2406.
Lee, H.J., Zhang, P., Bravman, J.C., 2003. Tensile failure by grain thinning in micromachined aluminum thin film. J. Appl. Phys. 93, 1443–1451.
Li, T., Huang, Z.Y., Lacour, S.P., Wagner, S., Suo, Z., 2004. Stretchability of thin metal films on elastomer substrates. Appl. Phys. Lett. 85, 3435–3437.
Li, T., Huang, Z.Y., Xi, Z.C., Lacour, S.P., Wagner, S., Suo, Z., 2005. Delocalizing strain in a thin metal film on a polymer substrate. Mech. Mater. 37, 261–273.
Macionczyk, F., Bruckner, W., 1999. Tensile testing of AlCu thin films on polyimide foils. J. Appl. Phys. 86, 4922–4929.
Niordson, F.I., 1965. A unit for testing materials at high strain rates. Exp. Mech. 5, 29–32.
Pashley, D.W., 1960. A study of the deformation and fracture of single-crystal gold films of high strength inside an electron microscope. Proc. Roy. Soc. Lond. A 255, 218–231.
Rivlin, R.S., 1982. Bifurcation in an elastic plate on a rigid substrate. Int. J. Solids Struct. 18, 411–418.
Shenoy, V.B., Freund, L.B., 1999. Necking bifurcations during high strain rate extension. J. Mech. Phys. Solids 47, 2209–2233.
Steif, P.F., 1986. Periodic necking instabilities in layered plastic solids. Int. J. Solids Struct. 22, 1571–1578.
Stören, S., Rice, J.R., 1975. Localized necking in thin sheets. J. Mech. Phys. Solids 23, 421–441.
Treloar, L.R.G., 1948. Stresses and birefringence in rubber subjected to general homogeneous strain. Proc. Phys. Soc. 60, 135–144.
Wagner, S., Lacour, S.P., Jones, J., Hsu, P.I., Sturm, J.C., Li, T., Suo, Z., 2005. Electronic skin: Architecture and components. Physica E 25, 326–334.
Xiang, Y., Chen, X., Vlassak, J.J., 2002. The mechanical properties of electroplated Cu thin films measured by means of the bulge test techniques. Mater. Res. Soc. Symp. Proc. 695, L4.9.
Xiang, Y., Li, T., Suo, Z., Vlassak, J.J., 2005. High ductility of a metal film adherent on a polymer substrate. Appl. Phys. Lett., submitted for publication.
Yu, D.Y.W., Spaepen, F., 2003. The yield strength of thin copper films on Kapton. J. Appl. Phys. 95, 2991–2997.